



# **Geophysical Research Letters**

#### RESEARCH LETTER

10.1029/2021GL094531

#### **Key Points:**

- Different models of Cenozoic subduction history in South Asia imply distinctive origins for the Tethyan–Greater Himalayan sequences
- Quantitively reproducing the Tethyan-Greater Himalayan mass helps constrain the Cenozoic subduction history in South Asia
- Both the Intra-oceanic Arc and Terrane models, but not the Greater India model, could have been operating during the Cenozoic subduction

#### **Supporting Information:**

Supporting Information may be found in the online version of this article.

#### Correspondence to:

L. Liu and Y.-G. Xu, ljliu@illinois.edu; yigangxu@gig.ac.cn

#### Citation:

Liu, L., Liu, L., & Xu, Y.-G. (2021). Intermittent post-Paleocene continental collision in South Asia. *Geophysical Research Letters*, 48, e2021GL094531. https://doi.org/10.1029/2021GL094531

Received 26 MAY 2021 Accepted 27 JUN 2021

# **Intermittent Post-Paleocene Continental Collision in South Asia**

Liang Liu<sup>1,2,3</sup>, Lijun Liu<sup>1</sup>, and Yi-Gang Xu<sup>2,3</sup>

<sup>1</sup>Department of Geology, University of Illinois at Urbana-Champaign, Urbana, IL, USA, <sup>2</sup>State Key Laboratory of Isotope Geochemistry and CAS Center of Excellence in Deep Earth Science, Guangzhou Institute of Geochemistry, Chinese Academy of Sciences, Guangzhou, China, <sup>3</sup>Southern Marine Science and Engineering Guangdong Laboratory (Guangzhou), Guangzhou, China

**Abstract** Three different conceptual models have been proposed for the Cenozoic subduction style in South Asia, including Greater India, Intra-oceanic Arc, and Continental Terrane (or Greater Indian basin). Since these models imply distinctive origins for the Tethyan–Greater Himalayan (TGH) sequences, for example, as a relic of the subducted Greater India or Gondwana–affiliated continental terrane, quantitively reproducing the relic TGH crustal mass with numerical models could help further constrain the debated Cenozoic subduction history between India and Eurasia. Based on the modeling results, we show that the subducted plate since the Paleocene should consist of a significant oceanic portion that is,  $\sim$ 1,000 km long for the Intra-oceanic Arc model and up to 2,000 km long for the Terrane model. Our results do not support the existence of a continuous >3,000 km long continental Greater India before the early Eocene collision in South Asia.

**Plain Language Summary** Approximately 55 million years ago, the Indian Subcontinent was in the Southern Hemisphere, >3,000 km away from Tibet. However, it remains unknown what tectonic units were between them. Previous studies suggest that this region was composed of either pure land or with parts being oceans. By now, this region has mostly foundered into the deep Earth, with its surface relics forming the Himalayan Mountains. Because land and ocean contribute differently to the relic materials, the mass of the Himalayan Mountain can provide essential information about this lost tectonic region. This study uses numerical models to replicate the relic Himalayan mass while evaluating the earlier proposed models. We found that to match the Himalayan mass, the region between Tibet and India ~55 million years ago could not be purely continental and should include >1,000 km long oceanic plate.

#### 1. Introduction

As the most extensive and highest landmass on Earth, the Tibetan Plateau has had a profound influence on the evolution of regional to global climate systems, the continental-scale drainage evolution, and biota history in South Asia since ca.  $55 \pm 5$  Ma (Ding et al., 2016; Molnar et al., 1993; Hu et al., 2016; Kapp & DeCelles, 2019). The formation of Tibetan Plateau is frequently related to the Cenozoic Indo–Eurasian collisional orogeny, during which the Gondwana–affiliated terranes continuously amalgamated onto the Eurasian plate south of the Yalu Suture Zone (YSZ; Gibbons et al., 2015; Kapp & DeCelles, 2019; Wu, 2008; Yin & Harrison, 2000). However, the exact style of post-Paleocene subduction/collision history in this region is still heavily debated. Consequently, it is difficult to quantify the Tibetan Plateau formation and its profound tectono-climatic effects (Molnar et al., 2010; Spicer et al., 2003).

A gradual convergence in recent studies is that the earliest Cenozoic collision at southern Eurasia or northern India occurred at ca.  $55 \pm 5$  Ma, evidenced in the appearance of exotically sourced sediments in the Himalayan sequences (Ding et al., 2016; Garzanti, 2019; Hu et al., 2016; Kapp & DeCelles, 2019; Yin, 2006). However, the subsequent subduction history remains elusive, where proposed models broadly fall into three categories. (a) Greater India model (Figures 1a and 1d), where continuous continental collision with Eurasia consumed >3,000 km of continental lithosphere (Ali & Aitchison, 2005; Lee & Lawver, 1995). (b) Intra-oceanic Arc model (Figures 1b and 1e; Aitchison et al., 2007; Gibbons et al., 2015; Kapp & DeCelles, 2019; Martin et al., 2020). In this case, a miniature Greater India ( $\sim$ 1,350–2,150 km long) collided with an intra-oceanic arc instead of Eurasia first, and its collision with Eurasia started at ca. 45–40 Ma

© 2021. American Geophysical Union. All Rights Reserved.

LIU ET AL. 1 of 10



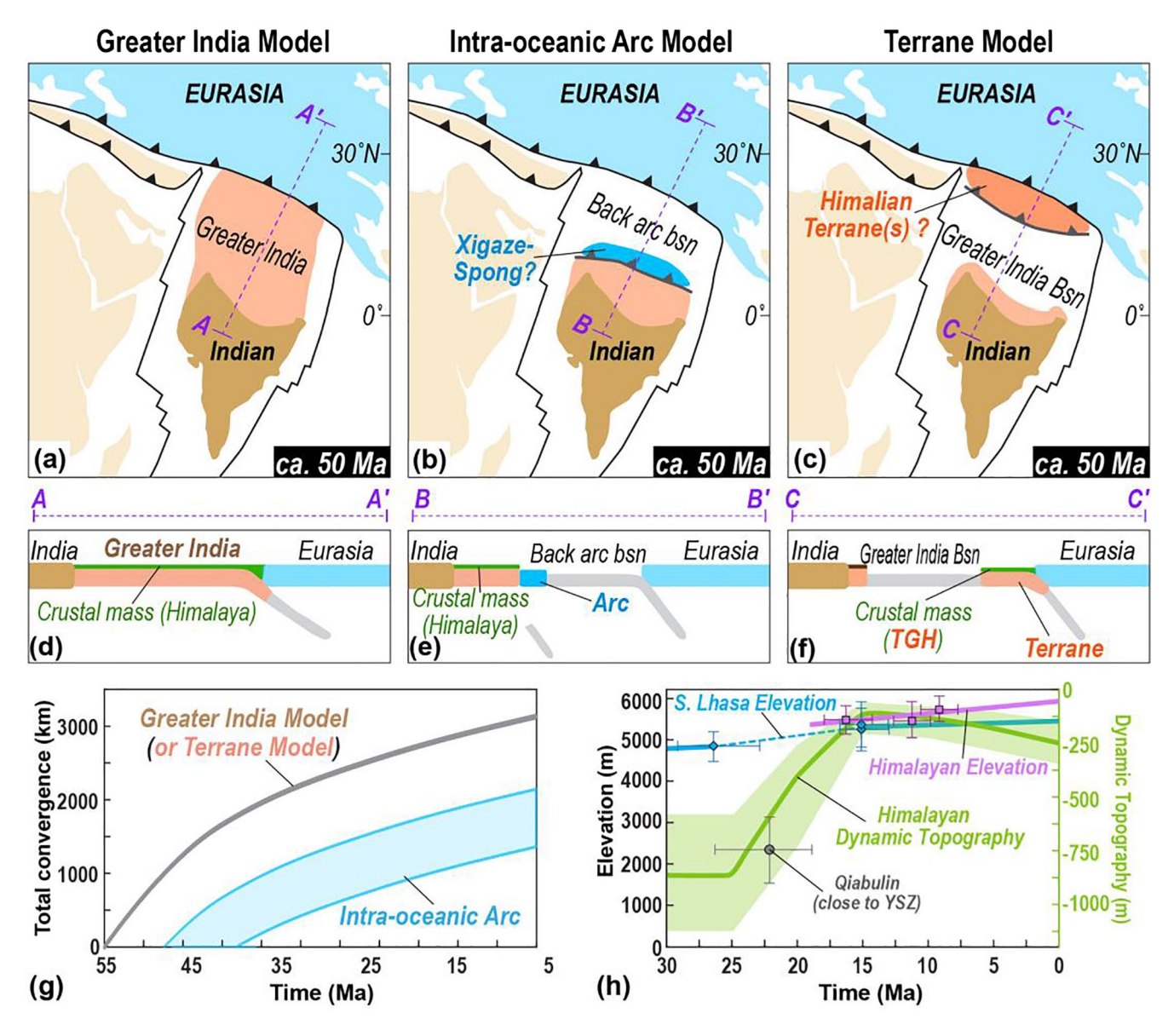


Figure 1. End-member models for the Indo-Eurasian Orogeny. (a) Greater India model (Ali & Aitchison, 2005; Lee & Lawver, 1995). The Greater Indian plate is composed of the present-day Indian Subcontinent (IS) and a >3,000 km long continental extension to its north. (b) Intra-oceanic arc model. A key feature is that the Xigaze-Spong forearc separated from Eurasia during a ca. 90–70 Ma rifting event (Kapp & DeCelles, 2019). This model implies the contiguous continental subduction started at ca. 45–40 Ma, after subduction of the back-arc. The intra-oceanic arc could also be the predecessor of the Kohistan-Ladakh Arc (Martin et al., 2020; van Hinsbergen et al., 2019). (c) Terrane model (or Greater Indian Basin model; van Hinsbergen et al., 2012, 2019). It implies that the terrane(s) departed from the Gondwana during the Cretaceous (ca. 120–65 Ma) and collided with Eurasia at ca. 55 Ma, following which the young oceanic plate (ca. 45–35 Myr crust) subducted beneath Eurasia until ~20 Ma when the IS finally collided with Eurasia. (d-f) Schematic cross-sections showing the subduction process along transects in (a-c). TGH: Tethyan-Greater Himalaya. The corresponding model setups are in Figure S1. (g) Cumulative convergence between the IS and Eurasia over time (see Figure S2 for the convergence rates used). The blue shaded trend marks the estimated length (1,350–2,150 km) of the subducted continental plate north of IS for the Intra-oceanic Arc model (Martin et al., 2020). (h) History of paleo-elevation (Ding et al., 2017) and dynamic topography (Husson et al., 2014) in the regions close to the Yalu Suture Zone (YSZ). Blue circles with error bars mark observational constraints for southernmost Lhasa and magenta ones for Himalaya. The pre-20 Ma paleo-elevation of these regions is still debatable, shown by the contrasting proxies (gray and blue circles before 20 Ma) of paleo-elevation (DeCelles et al., 2011; Ding et al., 2017; Ingalls et al., 2020; Kapp & DeCelles, 2019).

(Kapp & DeCelles, 2019). In these first two models, the Himalayan sequences represent scraped-off crust from the subducted Greater India. (c) Terrane model (or Greater Indian Basin model; Figures 1c and 1f; van Hinsbergen et al., 2012, 2019), where a Gondwana-affiliated terrane collided with Eurasia starting ~55 Ma, after ~40–35 Myr of oceanic subduction, with the relic terrane crust forming the Tethyan and Greater

LIU ET AL. 2 of 10



Himalaya (TGH). In all three models, Indian subduction started ca. 20–15 Ma (Kapp & DeCelles, 2019; van Hinsbergen et al., 2012, 2019).

One key reason behind these debates is the uncertainty (>10-degree) in the paleo-latitude of the orogen-generating continental blocks (e.g., Tethyan Himalaya; Huang et al., 2017; Martin et al., 2020; Parsons et al., 2020; Rowley, 2019; van Hinsbergen et al., 2012, 2019). In a recent review, Parsons et al. (2020) evaluated the above three models against the sedimentary and structural records close to the YSZ, as well as seismic tomography below the Indo–Eurasian Orogen. However, they concluded that all three models have their respective lines of observational support and that their considered data constraints cannot effectively distinguish these models.

A potential solution for differentiating these three models is through evaluating the crustal mass balance of the TGH. As noted above, the three models imply distinctive origin and evolution of the TGH crust (Figure 1). In the Terrane model, the source for the TGH is a narrow (e.g., <500 km long) continental terrane (van Hinsbergen et al., 2019). However, in both the Greater India and the Intra-oceanic Arc models, the parental continent is the subducted Greater India, whose total length is >3,000 km and 1,350-2,150 km, respectively (Kapp & DeCelles, 2019; Martin et al., 2020). This broad range (from <500 to >3,000 km) of subducted crustal length implies that the observed TGH crustal mass could be an essential constraint for further understanding the Cenozoic subduction history in South Asia.

Along this line, Yakovlev and Clark (2014) proposed that the >3,000 km long Greater India should have a thin (29–23 km) crust (Singh et al., 2017; Zhang & Klemperer, 2010). van Hinsbergen et al. (2019) stated similarly that the preserved Himalayan crustal mass is much less (>70%) than implied in the Greater India model. In these two studies, the researchers mainly recognized surface erosion as the dominant reason that caused crustal loss. Numerical modeling suggests that additional crustal losses could occur if the lower continental crust could decouple from the middle-upper crust such that it can subduct with the underlying lithospheric mantle (Capitanio et al., 2010; Liu et al., 2021). Another often overlooked factor is subduction erosion, during which the upper-plate's crust gets entrained at the trench, or scraped off at the base by the down-going slab (Kay et al., 1991; Stern, 2011). Given these uncertainties and assumptions, both the initial length and subsequent shortening of the TGH crust need to be revisited.

Here, we evaluate the final TGH crustal mass using numerical models that consider different scenarios of overriding and subducting plates to better understand the post-Paleocene subduction in South Asia. Key observational constraints include (a) the present-day width (~150–350 km) of TGH (cf. Singh et al., 2017), and (b) its average crustal thickness (~55–65 km; Singh et al., 2017; Zhang & Klemperer, 2010). According to previous studies, the TGH elevation reached the present value no later than ca. 20–15 Ma (DeCelles et al., 2011; Ding et al., 2017; Ingalls et al., 2020), since when the contribution of dynamic topography has been negligible (<200 m; Husson et al., 2014; Figure 1h). Therefore, the paleo-elevation of the TGH should mostly follow crustal isostasy during this history, implying that the TGH crust has attained the present thickness (and possibly width as well) since the Early Miocene at the latest. We suggest that physically plausible numerical models concerning the Indo–Eurasian Orogeny should match these two basic TGH crustal properties.

#### 2. Method

We present a total of 166 simulations (Table S1) that cover the three different scenarios of Indo-Eurasian Orogeny (Figure 1) in order to evaluate the evolution of TGH crustal mass. We use a MATLAB-based package to carry out 2-D numerical experiments (Hasenclever, 2010; Liu et al., 2018a, 2018b). This package is based on the Lagrangian-type finite element code MILAMIN (Dabrowski et al., 2008). It has a free surface on the top (Andrés-Martínez et al., 2015) and has been benchmarked with a free subduction study (Liu et al., 2018a). A triangular mesh is adaptively generated/regenerated according to the distribution of materials on tracers (Liu et al., 2018a, 2018b).

LIU ET AL. 3 of 10

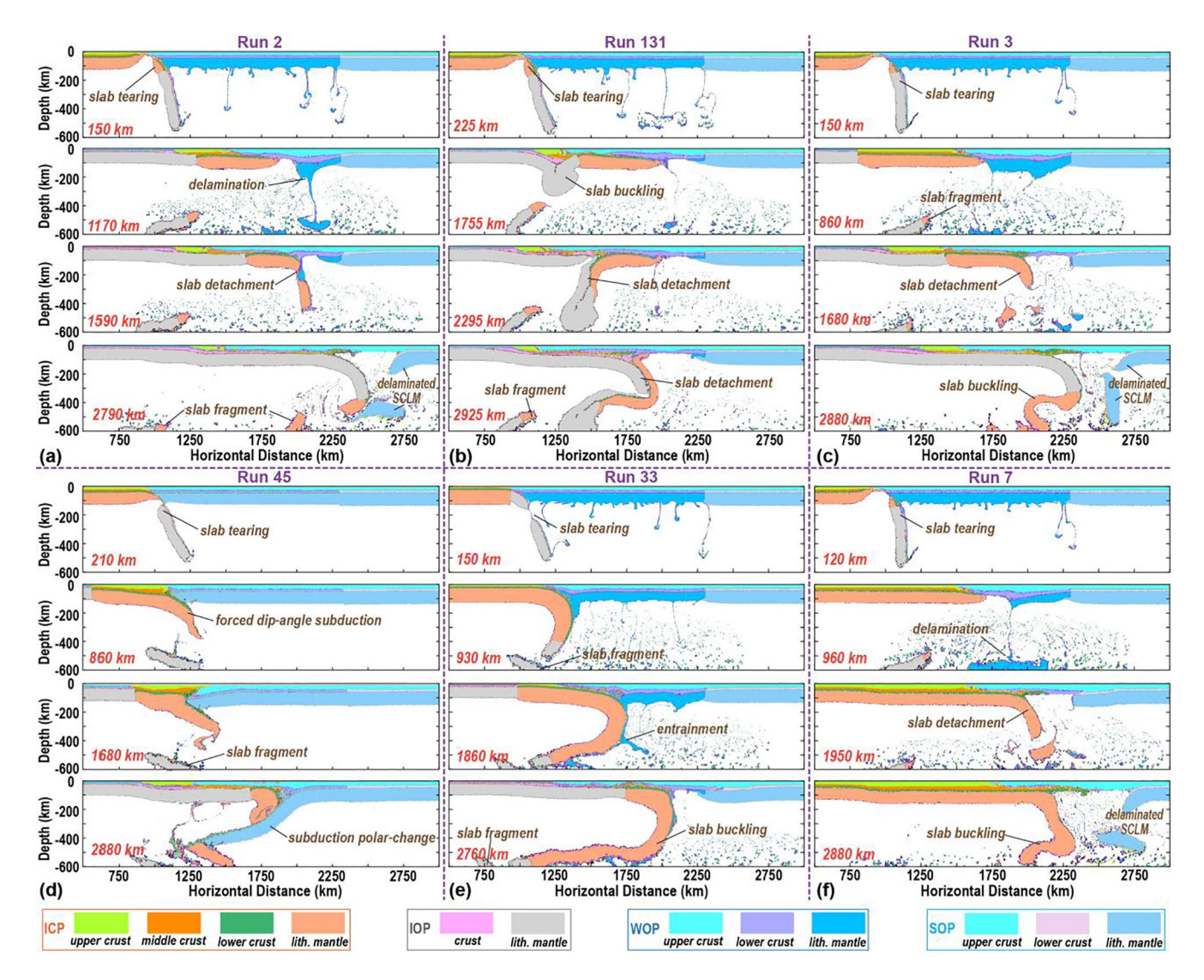


**Figure 2.** Material evolution in several representative models. (a–f) snapshots of the material evolution in Runs 2, 131, 3, 45, 33, and 7 (Table S1). The words in red demonstrate the amount of cumulative convergence in each snapshot. Lith. mantle-lithospheric mantle. The convergence rate in Run 131 is 9 cm/yr, and that in other models is 6 cm/yr. Summary for the key variables (Tables S1 and S2). Run 2: the incoming continental plate (ICP) is initially 600 km long, its crust is 40 km thick, the yielding stress for the weak overriding plate (WOP) lithospheric mantle is capped at 50 MPa, and that for the strong overriding plate (SOP) is capped at 200 MPa; the compositional density for the ICP lithospheric mantle ( $\rho_{TM}$ ) is 3,370 kg/m<sup>3</sup>. Run 131: same as Run 2, except that the yielding stress for the SOP lithospheric mantle is from Equation S6 without a cap value, and  $\rho_{TM}$  is 3,340 kg/m<sup>3</sup>. Run 3: same as Run 2, but the ICP is 900 km long. Run 45: same as Run 2, except that the ICP is 900 km long, and the overriding plate is uniformly strong (SOP, Table S2). Run 33: Same as Run 2, except that the ICP is 1,500 km long, and its initial crustal thickness is 20 km. Run 7: same to Run 2, but the incoming plate is entirely continental (Figure S1).

# 2.1. Model Setup

The 2D model box is 3,500 km wide  $\times$  1,000 km deep. It has four to six compositional domains (Figures 2, S1 and S3): (a) asthenosphere, (b) proceeding oceanic slab, (c) weak overriding plate (WOP), (d) strong overriding plate (SOP), (e) incoming continental plate (ICP), and (f) incoming oceanic plate (IOP). The IOP is 40 Myr old, mimicking the young back-arc basin formed before ca. 55 Ma (Kapp & DeCelles, 2019; van Hinsbergen et al., 2012, 2019). In Greater India models (Figure 1a), the incoming plate is purely continental. Intra-oceanic Arc models (Figure 1b) are the same as Greater India models except with a 1,350–2,150 km total convergence. Most Terrane models (Figure 1c) assume one single terrane (Table S1), from which the TGH results. We further show that Indian subduction does not alter the evolution of TGH crust (Figure S4), so this part of the subduction history is not considered in most other Terrane models. More model parameters are in Table S2.

LIU ET AL. 4 of 10



#### 2.2. Key Variables in the Numerical Models

In order to objectively evaluate the different models for Indo-Eurasian Orogeny (Tables S1 and S2), we consider the following key variables:

- 1. ICP crustal thickness is critical for terrane accretion (Yakovlev Clark, 2014). However, this property is poorly constrained, so we systematically tested its values, including 40, 30, and 20 km.
- 2. Upper plate delamination, a process proposed to have occurred after ca. 55 Ma (Chung et al., 2005; Platt & England, 1994) and could have influenced the TGH evolution. Here, we simulated different scenarios with an overriding plate that promotes or prohibits delamination.
- 3. Presence of a weak ICP mid-crustal layer, due to possible dehydration or melting of amphibole-rich minerals (Beaumont et al., 2001). We consider both a weak ( $<10^{20}$  Pa·s) and strong ( $>10^{22}$  Pa·s) ICP middle crust that results in distinct deformation behaviors upon subduction (<100 km; Figure S3).
- 4. Total convergence (Figure 1). Here, we run all models till the convergence reaches >3,000 km (Figure 1g). We followed the previous studies (Kelly et al., 2016; Li et al., 2016) using a constant convergence rate of 6, 9, or 12 cm/yr.
- 5. Buoyancy of ICP lithosphere. As shown in Liu et al. (2021), the ICP buoyancy significantly affects the continental subduction style. We further tested this effect by varying the length and density of the ICP lithospheric mantle.

#### 3. Results

Through testing a wide range of model parameters (Figures 2–4, Tables S1 and S2), we attempt to identify the conditions for the conceptual models to match TGH observational constraints (Figure 1).

#### 3.1. Typical Evolution of the Incoming Plate

Figure 2 outlines the typical ICP behaviors of these numerical models (more results in Figures S5 and S10). We observe the following model configurations that are consistent with those from previous studies, which also acts as a model validation:

- 1. A weak overriding plate experiences delamination upon ICP subduction (Figures 2a–2f, and S11; Gray & Pysklywec, 2012; Li et al., 2016).
- 2. Inadequate ICP buoyancy, for example, due to a thin crust (20 km), results in steep subduction (Figure S11; Liu et al., 2021). This process can entrain the weak overriding lithosphere (Figures 2e, S11, and S12; Kelly et al., 2016, 2020; Li et al., 2016).
- 3. If the overriding plate is viscously strong, the ICP also experiences high-angle subduction, which eventually leads to a reversal of subduction polarity (Figures 2d, and S7–S8 and Chen et al., 2017).
- 4. Peeling off of the SOP happens with the presence of a weak crustal layer and upward Asthenospheric intrusion (Figures 2a–2f, and S5–S6; Liu et al., 2018a).
- 5. ICP subduction, together with the delamination/subduction of the overriding plate, can reproduce the present-day seismic images beneath the Tibetan Plateau (Figures 2a–2f vs. 2d and S5–S10; Chen et al., 2017; Kelly et al., 2016, 2020; Li et al., 2016).

Besides the above model behaviors that are similar to previous reports, we also observe some new features. For example, the subduction-entrained lithospheric mantle can either be parts of the overriding plate or the incoming plate (Figures 2b, vs. 2e). Unlike the scenario in Liu et al. (2021), the incoming oceanic plate here is young (thus buoyant), according to multiple previous studies (Kapp & DeCelles, 2019; van Hinsbergen et al., 2019). This buoyant oceanic plate does not have enough density contrast from the nearby continental terrane, leading to continuous flat subduction (Figures 2a–2c and 2) instead of a new subduction zone behind the terrane (Liu et al., 2021). This behavior is also related to the fact that we did not incorporate a weak zone between the ocean and continental portions within the incoming plate (Liu et al., 2021; Zhong & Li, 2020). Observationally, a single stable trench within South Asia as modeled here is consistent with the geologic records (Kapp & DeCelles, 2019).

LIU ET AL. 5 of 10



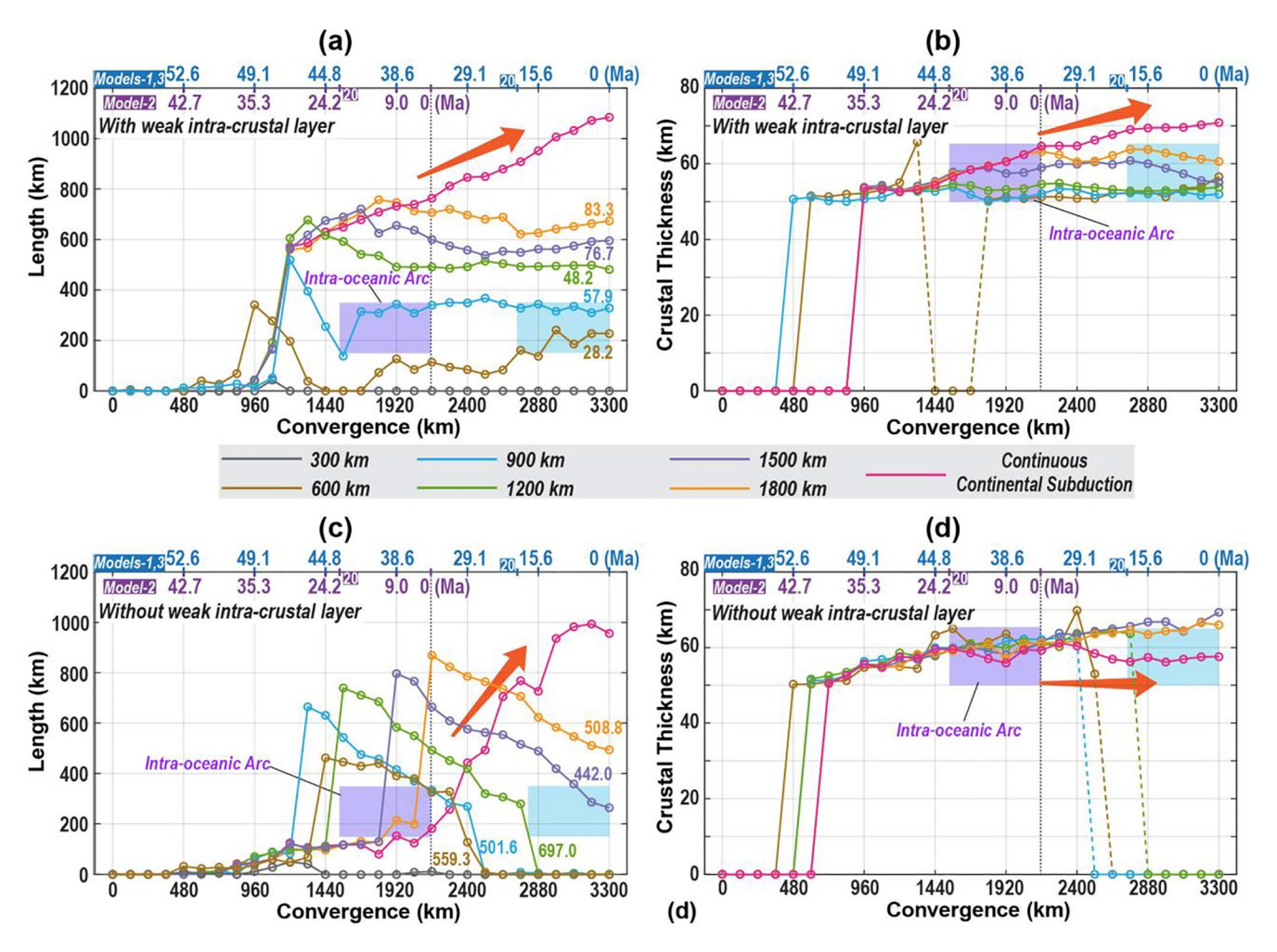


Figure 3. Evolution of the relic crust (only the portion thicker than 50 km) in Runs 1–14 (Table S1). (a) Relic crustal width in Runs 1–7, where the incoming continental plate (ICP) develops a weak middle crust once approaching the trench (<100 km). The number close to each line illustrates the average volume (or area of the 2D cross-section)-decreasing rate for the relic crust (or subduction-erosion rate, in km³/km/Myr), during the incoming oceanic plate (IOP) subduction after ~38 Ma. (b) Relic crustal thickness in Runs 1–7. In Run 7 (pink lines). The progressively increasing width and thickness of the accreted crust with total convergence (red arrows) are similar to those in Kelly et al. (2020). (c) Relic crustal width in Runs 8–14, where the ICP does not have a weak middle crust. (d) Relic crustal thickness in Runs 8–14. Model 1-Greater India model. Model 2-Intra–oceanic Arc model. Model 3-Terrane model. In all these models, the initial ICP crust is 40 km thick, and the overriding plate is weak and delaminates during ICP subduction. In Run 14 (pink lines), the quasi-steady thickness but increasing width of the accreted crust after a total convergence of ~1,500 km are consistent with those in Li et al. (2016). In each panel, the present-day corresponds to total convergence of 3,300 km for Greater India and Terrane models, and of 2,150 km for Intra-oceanic Arc models (Figure 1). The corresponding geological time is also shown, where the ages in purple are for Intra-oceanic Arc models, and those in blue are for the other two types of models. The 20–0 Ma period corresponds to a total convergence of ~550 km (Figure 1g), shown as blue and purple shaded boxes, which provides a lower limit for the observationally inferred duration of the stable TGH crustal thickness (Figure 1h). The present-day TGH crust measures ~50–65 km thick and 150–350 km wide (North-South), thus defining the vertical dimension of the purple and blue boxes.

#### 3.2. Relic Crust in Numerical Models

In models for Greater India and Intra-oceanic Arc subduction, we approximate the >50 km thick relic crust as the TGH. This is because, according to observation, the TGH crust is 50–65 km thick while the Lesser Himalaya is generally thinner than 50 km (Singh et al., 2017; Zhang & Klemperer, 2010). In the Terrane models, the relic terrane crust approximates the TGH (van Hinsbergen et al., 2019).

As shown in Figure 3 (and Figures S12–S16), the results, which strongly depend on the ICP crustal rheology, primarily fall into two categories. (a) With a weak ( $<10^{20}$  Pa·s) ICP middle crust, the thickness of the relic crust in the Terrane models (initial ICP length <1,800 km) becomes stable after  $\sim1,900$  km of total convergence (Figure 3b). In contrast, this value keeps increasing in the other two types of models (magenta lines) due to continuous continental subduction (Figures 3a–3b). (b) In the absence of a weak ICP middle crust

LIU ET AL. 6 of 10

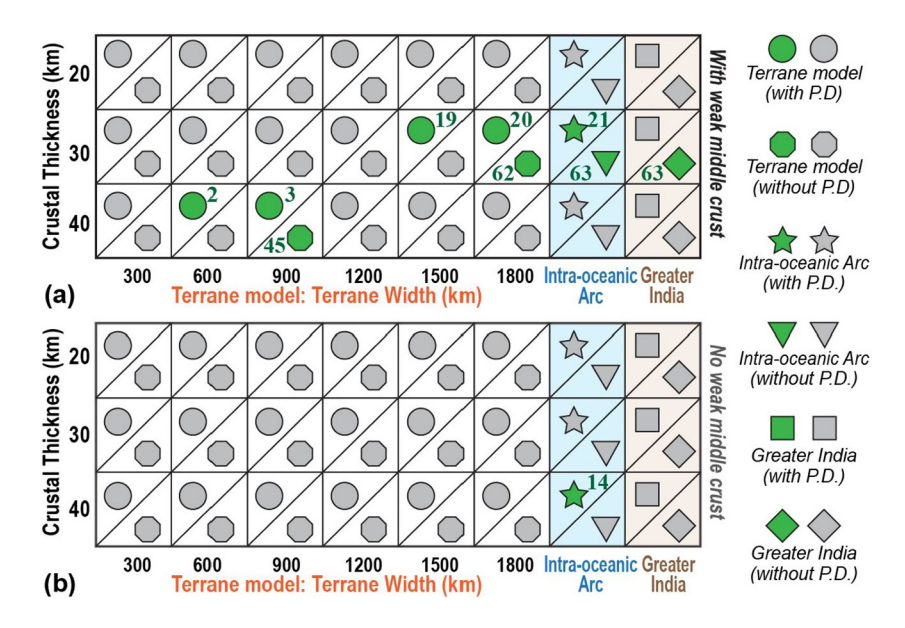


**Figure 4.** Checkbox summary of key model results. (a) Models with a weak incoming continental plate (ICP) middle crust. (b) Models without a weak ICP middle crust. The green and gray colors illustrate models that do or do not match the observations, respectively. The run numbers for models matching observations are in thick green font, and those for other models are in Table S3. P.D.: precedent delamination, which describes the weak overriding plate delamination (e.g., within the Tibetan block).

that also decouples the subduction interface, subduction erosion is much more prominent ( $\sim$ 450–700 km<sup>3</sup>/km/Myr in Figure 3c vs. <100 km<sup>3</sup>/km/Myr in Figure 3a) throughout the modeling history. This is illustrated by the rapidly decreasing crustal length in Terrane models after terrane subduction completes (with convergence >1,500 km), while the relic crust only slowly thickens (Figures 3c and 3d). In the other two types of models, the relic crustal length rapidly increases after  $\sim$ 1,500 km of convergence (Figure 3c), but its thickness remains largely stable (Figure 3d). More sensitivity tests are in Figures S17–S28.

#### 3.3. Best Fit Models

The above models permit a re-evaluation of the three different conceptual models (Figure 1). The Greater India model (Figure 1a), for the most promising scenario (Figure S15), could only match TGH constraints marginally well, where the ICP crust should be thin (30 km), develop a weak middle crust during collision/subduction, and have a highly viscous ( $>10^{22}$  Pa·s) overriding plate to prevent delamination (the green diamond in Figure 4a). However, most of these conditions seem inconsistent with the current understanding (see Section 4.2 for more reasoning). The Intra-oceanic Arc model has three possible scenarios, all with a marginal match to data, where the ICP crust should be 30 km thick with upper-plate delamination or 40 km without upper-plate delamination (Figures 3 and 4, S12 and S15). Terrane models could most comfortably match data, also with the largest number (six) of possible scenarios. In these cases, the only requirement is that the ICP needs to develop a weak middle crust during collision/subduction (Figures 3 and 4, S12 and S14).

#### 4. Discussion and Conclusion

#### 4.1. Limitations of the Numerical Models

In our numerical simulations, surface erosion, which can also alter the relic crustal mass (van Hinsbergen et al., 2019), is not considered. According to the exhumation rate for the Himalayan granitoid (Tremblay et al., 2015), the Himalayan crust exhumated as much as 6 km after ca. 45 Ma, the time when the three different models start to diverge. However, we suggest that this value is within the uncertainty of the present-day TGH crustal thickness and that a 6-km change in crustal thickness would not change our main

LIU ET AL. 7 of 10



results (Figures 3 and 4). We also note that the potential occurrence of lateral extrusion may further affect the understanding of North-South mass distribution close to the east and west Himalayan syntaxes after  $\sim$ 20 Ma (Capitanio et al., 2015; Li et al., 2013). In this case, our 2D models mainly provide constraints for the post-Paleocene subduction in regions away from the Himalayan syntaxes.

#### 4.2. Implications on Cenozoic South Asian Subduction

In the presented models, the initial/boundary conditions followed previous studies of Indo-Eurasian Orogeny, as shown in their similar model results (Figures 2 and S11). The broad range of model parameters here could utilize additional geological observations as model constraints. For example, lithospheric delamination seems necessary in explaining the Eocene intraplate magmatism in Qiangtang and the Miocene ones in Lhasa and Songpan–Ganzi (Chung et al., 2005; Kapp & DeCelles, 2019). In the numerical models that lack upper-plate delamination, the lithosphere in the orogen is usually too thick (>150 km) for melt to form (Figures 2d and S7–S8 and S10). Since the only possible scenario of the Greater India model requires the absence of precedent upper plate delamination (Figure 4a), it violates the magmatic records, rendering the Greater India model tectonically implausible.

In addition, both the Greater India and Intra-oceanic Arc models require a >1,700 km long continental region with a thin ( $\sim$ 30 km) crust, which, in the former case, should be >3,000 km. However, this seems inconsistent with present-day observation, where continental crusts are usually thicker than 30 km (cf., Artemieva & Shulgin, 2019). The most extensive continental shelf with thin (30–35 km) crust abutting a craton is the one that extends  $\sim$ 1,500 km off the Siberian coast into the Arctic. This observation challenges the Greater India model the most. However, we cannot exclude the possibility of a slightly broader ( $\sim$ 1,700–2,150 km) continental shelf to the north of India for the Intra-oceanic Arc model (Run 21 in Figure 4). In comparison, the Terrane model requiring a 600–900 km long ICP crust with a typical (40 km) thickness is more consistent with the present-day continental distribution (Runs 2–3 in Figures 3 and 4), especially around the Cenozoic Indian Ocean basin where extensive continental shelf has been rare.

Finally, previous studies emphasized the presence of a weak intra-crustal layer as the main reason allowing the lower continental crust to subduct during the Indo–Eurasian convergence (Beaumont et al., 2001; Capitanio et al., 2010; Copley et al., 2011; Ingalls et al., 2016). Our numerical results further support this inference by showing that most scenarios that match the TGH constraints require a weak ICP middle crust (Figures 4a vs. 4b). In the models where the ICP develops a weak middle crust, the subduction erosion rate during the IOP subduction is  $\sim$ 30–80 km³/km/Myr (Figure 3), consistent with the previous estimates for global subduction zones (Stern, 2011). In contrast, in models without the weak ICP middle crust, the subduction erosion rate can be one order of magnitude greater (Figure 3). Therefore, a low-viscosity ICP middle crustal layer appears geologically relevant (Figures 3c, 3d, and 4b).

In conclusion, by comparing modeled versus observed TGH crustal properties, we propose that the subducted plate(s) beneath southern Eurasia since ca. 55 Ma should consist of (a) a moderately long ( $\sim$ 600–2,000 km) continental portion with 30–40 km thick crust, and (b) a >1,000 km long oceanic portion that did not contribute to TGH crustal growth. Consequently, our results suggest that both the Intra-oceanic Arc and Terrane models, but not the Greater India model, could have been operating Cenozoic subduction in South Asia.

### Acknowledgments

We acknowledge Fan Yang, two anonymous reviewers, and editor Lucy Flesch for constructive suggestions on the manuscript. L. Liu is jointly supported by UIUC and the Guangdong Provincial Post-doc Program, and acknowledges NSFC grant 41911530194. L. J. Liu acknowledges NSF grants EAR 1554554, 1565640, and the GeoThrust Foundation at UIUC. Y-G. Xu acknowledges NSFC grant 41688103 and the Chinese Academy of Sciences grant XDB18000000.

## **Data Availability Statement**

All figures and movies are produced by the equations in the supplements, together with initial/boundary conditions and model parameters given in the supplements. The numerical results for four typical models (Runs 3, 33, 56, and 131) and related plot scripts will be available at https://zenodo.org/.

#### References

Aitchison, J. C., Ali, J. R., & Davis, A. M. (2007). When and where did India and Asia collide? *Journal of Geophysical Research*, 112(B5). https://doi.org/10.1029/2006jb004706

Ali, J. R., & Aitchison, J. C. (2005). Greater India. Earth-Science Reviews, 72(3-4), 169-188. https://doi.org/10.1016/j.earscirev.2005.07.005

LIU ET AL. 8 of 10



- Andrés-Martínez, M., Morgan, J. P., Pérez-Gussinyé, M., & Rüpke, L. (2015). A new free-surface stabilization algorithm for geodynamical modelling: Theory and numerical tests. *Physics of the Earth and Planetary Interiors*, 246, 41–51. https://doi.org/10.1016/j.pepi.2015.07.003
- Artemieva, I. M., & Shulgin, A. (2019). Geodynamics of Anatolia: Lithosphere thermal structure and thickness. *Tectonics*, 38(12), 4465–4487. https://doi.org/10.1029/2019tc005594
- Beaumont, C., Jamieson, R. A., Nguyen, M. H., & Lee, B. (2001). Himalayan tectonics explained by extrusion of a low-viscosity crustal channel coupled to focused surface denudation. *Nature*, 414(6865), 738–742. https://doi.org/10.1038/414738a
- Capitanio, F. A., Morra, G., Goes, S., Weinberg, R. F., & Moresi, L. (2010). India–Asia convergence driven by the subduction of the Greater Indian continent. *Nature Geoscience*, 3(2), 136–139. https://doi.org/10.1038/ngeo725
- Capitanio, F. A., Replumaz, A., & Riel, N. (2015). Reconciling subduction dynamics during Tethys closure with large-scale Asian tectonics: Insights from numerical modeling. *Geochemistry, Geophysics, Geosystems*, 16(3), 962–982. https://doi.org/10.1002/2014gc005660
- Chen, L., Capitanio, F. A., Liu, L., & Gerya, T. V. (2017). Crustal rheology controls on the Tibetan plateau formation during India-Asia convergence. *Nature Communications*, 8(1), 1–8. https://doi.org/10.1038/ncomms15992
- Chung, S. L., Chu, M. F., Zhang, Y., Xie, Y., Lo, C. H., Lee, T. Y., et al. (2005). Tibetan tectonic evolution inferred from spatial and temporal variations in post-collisional magmatism. *Earth-Science Reviews*, 68(3–4), 173–196. https://doi.org/10.1016/j.earscirev.2004.05.001
- Copley, A., Avouac, J. P., & Wernicke, B. P. (2011). Evidence for mechanical coupling and strong Indian lower crust beneath southern Tibet. Nature, 472(7341), 79–81. https://doi.org/10.1038/nature09926
- Dabrowski, M., Krotkiewski, M., & Schmid, D. W. (2008). MILAMIN: MATLAB-based finite element method solver for large problems. *Geochemistry, Geophysics, Geosystems*, 9(4). https://doi.org/10.1029/2007gc001719
- DeCelles, P. G., Kapp, P., Quade, J., & Gehrels, G. E. (2011). Oligocene–Miocene Kailas basin, southwestern Tibet: Record of postcollisional upper-plate extension in the Indus-Yarlung suture zone. *Bulletin*, 123(7–8), 1337–1362. https://doi.org/10.1130/b30258.1
- Ding, L., Qasim, M., Jadoon, I. A., Khan, M. A., Xu, Q., Cai, F., et al. (2016). The India–Asia collision in north Pakistan: Insight from the U–Pb detrital zircon provenance of Cenozoic foreland basin. *Earth and Planetary Science Letters*, 455, 49–61. https://doi.org/10.1016/j.epsl.2016.09.003
- Ding, L., Spicer, R. A., Yang, J., Xu, Q., Cai, F., Li, S., et al. (2017). Quantifying the rise of the Himalaya orogen and implications for the South Asian monsoon. *Geology*, 45(3), 215–218. https://doi.org/10.1130/g38583.1
- Garzanti, E. (2019). The Himalayan Foreland Basin from collision onset to the present: A sedimentary–petrology perspective. *Geological Society, London, Special Publications*, 483(1), 65–122. https://doi.org/10.1144/sp483.17
- Gibbons, A. D., Zahirovic, S., Müller, R. D., Whittaker, J. M., & Yatheesh, V. (2015). A tectonic model reconciling evidence for the collisions between India, Eurasia and intra-oceanic arcs of the central-eastern Tethys. *Gondwana Research*, 28(2), 451–492. https://doi.org/10.1016/j.gr.2015.01.001
- Gray, R., & Pysklywec, R. N. (2012). Geodynamic models of mature continental collision: Evolution of an orogen from lithospheric subduction to continental retreat/delamination. *Journal of Geophysical Research*, 117(B3). https://doi.org/10.1029/2011jb008692
- Hasenclever, J. (2010). Modeling mantle flow and melting processes at Mid-Ocean ridges and subduction zones—development and application of numerical models (Doctoral dissertation). Staats-und Universitätsbibliothek Hamburg Carl von Ossietzky.
- Hu, X., Garzanti, E., Wang, J., Huang, W., An, W., & Webb, A. (2016). The timing of India-Asia collision onset–Facts, theories, controversies. *Earth-Science Reviews*, 160, 264–299. https://doi.org/10.1016/j.earscirev.2016.07.014
- Huang, W., Lippert, P. C., Jackson, M. J., Dekkers, M. J., Zhang, Y., Li, J., et al. (2017). Remagnetization of the Paleogene Tibetan Himalayan carbonate rocks in the Gamba area: Implications for reconstructing the lower plate in the India-Asia collision. *Journal of Geophysical Research: Solid Earth*, 122(2), 808–825. https://doi.org/10.1002/2016jb013662
- Husson, L., Bernet, M., Guillot, S., Huyghe, P., Mugnier, J. L., Replumaz, A., et al. (2014). Dynamic ups and downs of the Himalaya. *Geology*, 42(10), 839–842. https://doi.org/10.1130/g36049.1
- Ingalls, M., Rowley, D. B., Currie, B., & Colman, A. S. (2016). Large-scale subduction of continental crust implied by India–Asia mass-balance calculation. *Nature Geoscience*, 9(11), 848–853. https://doi.org/10.1038/ngeo2806
- Ingalls, M., Rowley, D. B., Currie, B. S., & Colman, A. S. (2020). Reconsidering the uplift history and peneplanation of the northern Lhasa terrane, Tibet. *American Journal of Science*, 320(6), 479–532. https://doi.org/10.2475/06.2020.01
- Kapp, P., & DeCelles, P. G. (2019). Mesozoic-Cenozoic geological evolution of the Himalayan-Tibetan orogen and working tectonic hypotheses. American Journal of Science, 319(3), 159–254. https://doi.org/10.2475/03.2019.01
- Kay, S. M., Mpodozis, C., Ramos, V. A., & Munizaga, F. (1991). Magma source variations for mid-late Tertiary magmatic rocks associated with a shallowing subduction zone and a thickening crust in the central Andes (28 to 33 S). Geological Society of America Special Paper, 265, 113–138. https://doi.org/10.1130/spe265-p113
- Kelly, S., Beaumont, C., & Butler, J. P. (2020). Inherited terrane properties explain enigmatic post-collisional Himalayan-Tibetan evolution. *Geology*, 48(1), 8–14. https://doi.org/10.1130/g46701.1
- Kelly, S., Butler, J. P., & Beaumont, C. (2016). Continental collision with a sandwiched accreted terrane: Insights into Himalayan–Tibetan lithospheric mantle tectonics? Earth and Planetary Science Letters, 455, 176–195. https://doi.org/10.1016/j.epsl.2016.08.039
- Lee, T. Y., & Lawver, L. A. (1995). Cenozoic plate reconstruction of Southeast Asia. Tectonophysics, 251(1-4), 85-138. https://doi.org/10.1016/0040-1951(95)00023-2
- Li, Z. H., Liu, M., & Gerya, T. (2016). Lithosphere delamination in continental collisional orogens: A systematic numerical study. *Journal of Geophysical Research: Solid Earth*, 121(7), 5186–5211. https://doi.org/10.1002/2016jb013106
- Li, Z. H., Xu, Z., Gerya, T., & Burg, J. P. (2013). Collision of continental corner from 3-D numerical modeling. *Earth and Planetary Science Letters*, 380, 98–111. https://doi.org/10.1016/j.epsl.2013.08.034
- Liu, L., Liu, L., & Xu, Y. G. (2021). Mesozoic intraplate tectonism of East Asia due to flat subduction of a composite terrane slab. Earth-Science Reviews, 214, 103505. https://doi.org/10.1016/j.earscirev.2021.103505
- Liu, L., Morgan, J. P., Xu, Y., & Menzies, M. (2018a). Craton destruction 1: Cratonic keel delamination along a weak midlithospheric discontinuity layer. *Journal of Geophysical Research*: Solid Earth, 123(11), 10–040. https://doi.org/10.1029/2017jb015372
- Liu, L., Morgan, J. P., Xu, Y., & Menzies, M. (2018b). Craton destruction 2: Evolution of cratonic lithosphere after a rapid keel delamination event. *Journal of Geophysical Research: Solid Earth*, 123(11), 10–069. https://doi.org/10.1029/2017jb015374
- Martin, C. R., Jagoutz, O., Upadhyay, R., Royden, L. H., Eddy, M. P., Bailey, E., et al. (2020). Paleocene latitude of the Kohistan–Ladakh arc indicates multistage India–Eurasia collision. *Proceedings of the National Academy of Sciences*, 117(47), 29487–29494. https://doi.org/10.1073/pnas.2009039117
- Molnar, P., Boos, W. R., & Battisti, D. S. (2010). Orographic controls on climate and paleoclimate of Asia: Thermal and mechanical roles for the Tibetan Plateau. *Annual Review of Earth and Planetary Sciences*, 38. https://doi.org/10.1146/annurev-earth-040809-152456

LIU ET AL. 9 of 10



- Molnar, P., England, P., & Martinod, J. (1993). Mantle dynamics, uplift of the Tibetan Plateau, and the Indian monsoon. *Reviews of Geophysics*, 31(4), 357–396. https://doi.org/10.1029/93rg02030
- Parsons, A. J., Hosseini, K., Palin, R., & Sigloch, K. (2020). Geological, geophysical and plate kinematic constraints for models of the India-Asia collision and the post-Triassic central Tethys oceans. *Earth-Science Reviews*, 208, 103084. https://doi.org/10.1016/j. earscirey.2020.103084
- Platt, J., & England, P. (1994). Convective removal of lithosphere beneath mountain belts-Thermal and mechanical consequences. *American Journal of Science*, 294(3). https://doi.org/10.2475/ajs.294.3.307
- Rowley, D. B. (2019). Comparing paleomagnetic study means with apparent wander paths: A case study and paleomagnetic test of the Greater India versus Greater Indian Basin hypotheses. Tectonics, 38(2), 722–740. https://doi.org/10.1029/2017tc004802
- Singh, A., Ravi Kumar, M., Mohanty, D. D., Singh, C., Biswas, R., & Srinagesh, D. (2017). Crustal structure beneath India and Tibet: New constraints from inversion of receiver functions. *Journal of Geophysical Research: Solid Earth*, 122(10), 7839–7859. https://doi.org/10.1002/2017jb013946
- Spicer, R. A., Harris, N. B., Widdowson, M., Herman, A. B., Guo, S., Valdes, P. J., et al. (2003). Constant elevation of southern Tibet over the past 15 million years. *Nature*, 421(6923), 622–624. https://doi.org/10.1038/nature01356
- Stern, C. R. (2011). Subduction erosion: Rates, mechanisms, and its role in arc magmatism and the evolution of the continental crust and mantle. *Gondwana Research*, 20(2–3), 284–308. https://doi.org/10.1016/j.gr.2011.03.006
- Tremblay, M. M., Fox, M., Schmidt, J. L., Tripathy-Lang, A., Wielicki, M. M., Harrison, T. M., et al. (2015). Erosion in southern Tibet shut down at ~10 Ma due to enhanced rock uplift within the Himalaya. *Proceedings of the National Academy of Sciences*, 112(39), 12030–12035. https://doi.org/10.1073/pnas.1515652112
- van Hinsbergen, D. J., Lippert, P. C., Dupont-Nivet, G., McQuarrie, N., Doubrovine, P. V., Spakman, W., & Torsvik, T. H. (2012). Greater India Basin hypothesis and a two-stage Cenozoic collision between India and Asia. *Proceedings of the National Academy of Sciences*, 109(20), 7659–7664. https://doi.org/10.1073/pnas.1117262109
- van Hinsbergen, D. J., Lippert, P. C., Li, S., Huang, W., Advokaat, E. L., & Spakman, W. (2019). Reconstructing Greater India: Paleogeographic, kinematic, and geodynamic perspectives. *Tectonophysics*, 760, 69–94. https://doi.org/10.1016/j.tecto.2018.04.006
- Wu, F. Y. (2008). Collapsed Himalayan-Tibetan orogen and the rising Tibetan Plateau. *Acta Petrologica Sinica*, 24, 1–30. (in Chinese with English abstract). https://doi.org/10.1007/s10114-007-6354-y
- Yakovlev, P. V., & Clark, M. K. (2014). Conservation and redistribution of crust during the Indo-Asian collision. *Tectonics*, 33(6), 1016–1027. https://doi.org/10.1002/2013tc003469
- Yin, A. (2006). Cenozoic tectonic evolution of the Himalayan orogen as constrained by along-strike variation of structural geometry, exhumation history, and foreland sedimentation. Earth-Science Reviews, 76(1-2), 1-131. https://doi.org/10.1016/j.earscirev.2005.05.004
- Yin, A., & Harrison, T. M. (2000). Geologic evolution of the Himalayan-Tibetan orogen. *Annual Review of Earth and Planetary Sciences*, 28(1), 211–280, https://doi.org/10.1146/annurey.earth.28.1.211
- Zhang, Z., & Klemperer, S. (2010). Crustal structure of the Tethyan Himalaya, southern Tibet: New constraints from old wide-angle seismic data. *Geophysical Journal International*, 181(3), 1247–1260. https://doi.org/10.1111/j.1365-246x.2010.04578.x
- Zhong, X., & Li, Z. H. (2020). Subduction initiation during collision-induced subduction transference: Numerical modeling and implications for the Tethyan evolution. *Journal of Geophysical Research: Solid Earth*, 125(2), e2019JB019288. https://doi.org/10.1029/2019jb019288

LIU ET AL. 10 of 10